ORIGINAL ARTICLE

Optimization of Intraventricular Radioactive Concentration for ^{13}N ammonia PET with Time-of-Flight Scanner: Simplified Phantom Study with Noise Equivalent Count Rate Analysis

Yoko Kaimoto, RT[1), 5)], Kenji Fukushima, MD, PhD[2)], Kazuko Kanaya, MT[1)], Masayasu Asanuma, RT[1)], Kaoru Aoba, RT[1)], Atsushi Yamamoto, MD, PhD[3), 4)], Risako Nakao, MD, PhD[4)], Koichiro Kaneko, MD, PhD[3)], Michinobu Nagao, MD, PhD[3)], and Koichi Chida, PhD[5)]

Received: November 17, 2022/Revised manuscript received: February 2, 2023/Accept: February 9, 2023
J-STAGE advance published: March 14, 2023

Abstract

***Background*: Myocardial blood flow quantification (MBF) is one of the distinctive features for cardiac positron emission tomography. The MBF calculation is mostly obtained by estimating the input function from the time activity curve in dynamic scan. However, there is a substantial risk of count-loss because the high radioactivity pass through the left ventricular (LV) cavity within a short period. We aimed to determine the optimal intraventricular activity using the noise equivalent count rate (NECR) analysis with simplified phantom model.**

***Methods*: Positron emission tomography computed tomography scanner with LYSO crystal and time of flight was used for phantom study. 150 MBq/mL of ^{13}N was filled in 10 mL of syringe, placed in neck phantom to imitate end-systolic small LV. 3D list-mode acquisition was repeatedly performed along radioactive decay. Net true and random count rate were calculated and compared to the theoretical activity in the syringe. NECR curve analysis was used to determine the optimal radioactive concentration.**

***Result*: The attenuation curves showed good correlation to the theoretical activity between 20 to 370, and 370 to 740 MBq (r^2=1.0 ± 0.0001, p<0.0001; r^2=0.99 ± 0.0001, p<0.0001 for 20 to 370, and 370 to 740, respectively), while did not over 740 MBq (p=0.62). NECR analysis revealed that the peak rate was at 2.9 Mcps, there at the true counts were significantly suppressed. The optimal radioactive concentration was determined as 36 MBq/mL.**

***Conclusion*: Simulative analysis for high-dose of ^{13}N using the phantom imitating small LV confirmed that the risk of count-loss was increased. The result can be useful information in assessing the feasibility of MBF quantification in clinical routine.**

Keywords: Cardiac PET, Input function, Myocardial flow, Myocardial perfusion, Noise equivalent counts ratio
Ann Nucl Cardiol 2023; 9 (1): 33–39

Myocardial blood flow (MBF) quantification is one of the premier techniques for cardiac positron emission tomography (PET), allowing non-invasive assessment of coronary microvascular endothelial function in addition to conventional qualitative visual assessments (1). In recent years, 3D mode acquisition and time-of-flight (TOF) technology have been widely introduced into clinical cardiac PET. These advanced technique have significantly improved signal-to-noise ratio by detecting an arrival of a pair of coincident photon, and offer higher counts rate (2). Namely, the image quality of cardiac PET has been upgraded due to higher sensitivity, while the issue of higher scatter fraction, random coincidence, and the count loss has been noticed (3). In general, kinetic models for MBF calculation employs the

DOI: 10.17996/anc.23-00178

1) Department of Radiological service, Tokyo Woman's Medical University, Tokyo, Japan
2) Department of Radiology and Nuclear Medicine, Fukushima Medical University, Fukushima, Japan
3) Department of Diagnostic Imaging and Nuclear Medicine, Tokyo Women's Medical University, Tokyo, Japan
4) Department of Cardiology, Tokyo Women's Medical University, Tokyo, Japan
5) Department of Health Sciences, Graduate School of Medicine, Tohoku University, Miyagi, Japan

estimated input function (IF) which is obtained from the time activity curve (TAC) in the cardiac chamber such as left ventricle, instead of blood sampling or measuring injected dose (1). TAC is generated from list mode acquisition of starting shorter frames and up to minutes for dynamic, static and gated images. However, the IF can be substantially influenced by the injected dose because high radioactivity passes through left ventricle in shorter period (4). Injected dose is proportional to the activity in the patient. Furthermore, the size of cardiac chamber is significantly small compared to that of western countries, indicating that it become critical issue especially in the patients with small heart which is frequently found in routine clinical practice in Japan (5).

The limited performance at higher activities in small volume is due to increasing counting losses and accidental coincidences, and it is natural to try to reduce the noise by injecting the patient with higher activities of perfusion tracer to increase the counting rate. The noise-equivalent counting rate (NECR) response curve, the estimation of unavoidable noise in the true coincidence data is mostly employed to minimize the relative data variance to obtain optimal injected dose (6, 7). NECR is typically assessed from simulations and actual measurements of radioactive concentration in phantoms, and the results should be adapted to humans (8). The National Electrical Manufacturers Association (NEMA) standard suggests a counting-rate measurement to provide a reasonable setting for PET in clinical studies for optimal injected dose based on NECR (9). Nevertheless, the NECR evaluation for cardiac PET in clinical setting for humans is quite varied, and less feasible to characterize this variability in patients. Several studies have simulated the IF measurement and myocardial uptake using original phantoms (4, 10). However, no established and feasible estimation for continuous measurements of intraventricular radioactive counts, especially with small-sized so far. Consequently, the precise evaluation of count-loss from intraventricular radioactivity is quite challenging because of estimating count-loss in small chamber with frequent motion is technically difficult.

In this study, we aimed to preliminary estimate the optimal activity to obtain the reproducible IF with minimized count-loss using a simplified phantom model imitating small left ventricle.

Materials and methods

PET/CT scanner

All data were obtained using the Biograph mCT scanner (Siemens Healthineer. Enlargen, Germany), a fully 3D TOF technique combined with a 64-slice computed tomography (CT) scanner. PET unit contains 4-rings based on 12 detector blocks in each module with a total of 32447 LYSO elements of $4.0 \times 4.0 \times 20$ mm crystals. The mCT enables axial FOV of 22.1 cm and trans axial field of view (FOV) of 70 cm. The ring diameter is 780 mm. The coincidence window is 4.1 ns. The TOF timing resolution is 540 ps. A sequential CT scan (120 kV, 20 mAs, 3 mm slice collimation) was acquired correction for CT attenuation correction. All emission data were acquired in 3D list-mode. The data was reconstructed with TrueX+TOF (ultra HD-PET), iteration 2, subsets 21, image size 200, and Gaussian 6 mm.

Phantom and acquisition protocol

Figure 1 showed a schematic presentation for PET acquisition. Oak Ridge Institute for Nuclear Studies standard thyroid uptake phantom (Kyoto-Kagaku Co., Ltd., Kyoto, Japan) was used in this study. The phantom has two large, interconnected holes to imitate thyroid. A 10 mL clear sterile evacuated vial (Steriscience, Inc.) filled with ^{13}N of approximately 150 MBq/mL was firstly measured by Curie-meter (IGC-3®, ALOKA Co., Ltd., Tokyo, Japan) prior to each set for PETCT acquisition, then placed in the hole on one side to simulate the smallest endo-systolic volume in female adopted from Japanese database of gated-single photon emission computed tomography (SPECT) study (11). Theoretical dose for each time point was computed by radio-active decay from initial measurement by Curie-meter. A single session (a combination of 60 sec acquisition and 60 sec standby) was repeated for 31 times in list mode collection. The examination was repeated for 6 days (6 sets). For data analysis, Syngo.via® VB30A_HF08 (Siemens Healthineer) was used to measure actual activity from PET acquisition. A spherical volume of interest was set as 4 mL, and to coverage the entire 10 mL vial with default threshold of 40%, and max radioactive concentration (Bq/mL) was measured for each single session. A decay curve was created from each of the 6 datasets and compared to the theoretical values based on the measured dose obtained from curie meter prior to PET acquisition. Estimated optimal dose was determined from the NECR generated from each set. The NECR was calculated as follows:

$$NECR = \frac{T^2}{T+S+2R},$$

where, T, S, and R stand for the true, scatter, and random count rates, respectively (7). A simple linear regression was employed to confirm the linearity between actual and theoretical values.

Results

An initial activity measured in curie meter was 1309.9 ± 76.0 MBq (1322.65, 1344.65, 1178.65, 1335.65, 1270.44, and 1397.63 MBq for the dataset of day 1 to day 6). Figure 2 showed the count-rate capabilities of the PET scanner for all 6 sets of acquisition. The plots of the graph varied over the

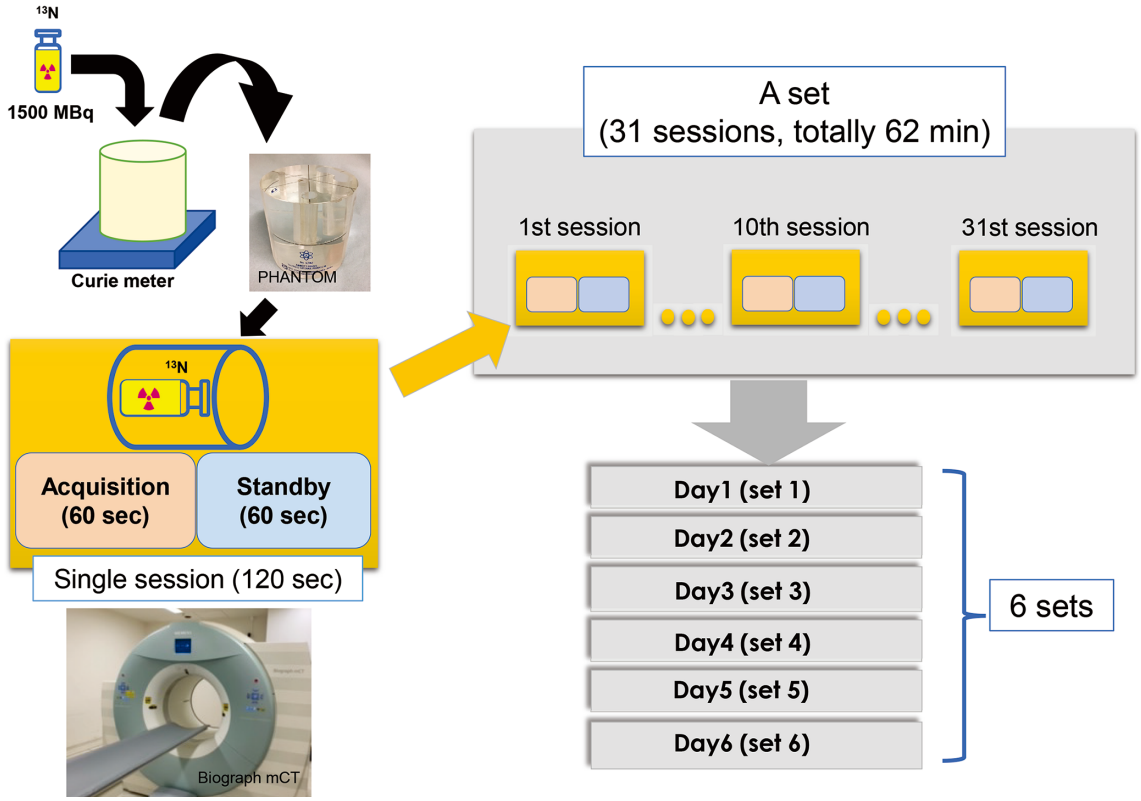

Figure 1 PET acquisition protocol for ^{13}N phantom study.

Schematic presentation for PET acquisition protocol. A 10 mL of vial imitating small left ventricle filled with approximately 1500 MBq of ^{13}N was measured by Curie-meter prior to PETCT acquisition for each set, then placed in the one side of the standard thyroid uptake phantom. A single session of PETCT scan consisted of a combination of 60 sec list-mode acquisition and 60 sec standby, and was repeated 31 times for a set, totally 62 min for each day. Theoretical dose for each time point was computed by ^{13}N radio-active decay from the firstly measured activity by curie meter. A single set was repeated for 6 days.

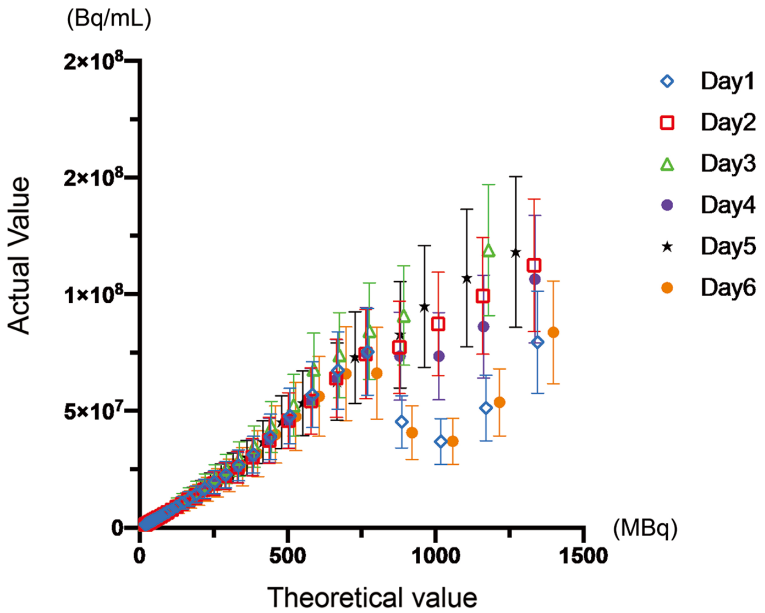

Figure 2 Comparison of measured and reference value for various ^{13}N dose.

The plots of measured and theoretical activity for each session were shown. X-axis indicated the theoretical activity estimated by the radioactive decay from the measured activity in the vial obtained by curie meter prior to PET scan. Y-axis indicated the measured radioactivity of the vial from the PET acquisitions. The plots apparently showed disagreement over the theoretical value of approximately 800 MBq, while they showed a good linearity the range below approximately 400 MBq.

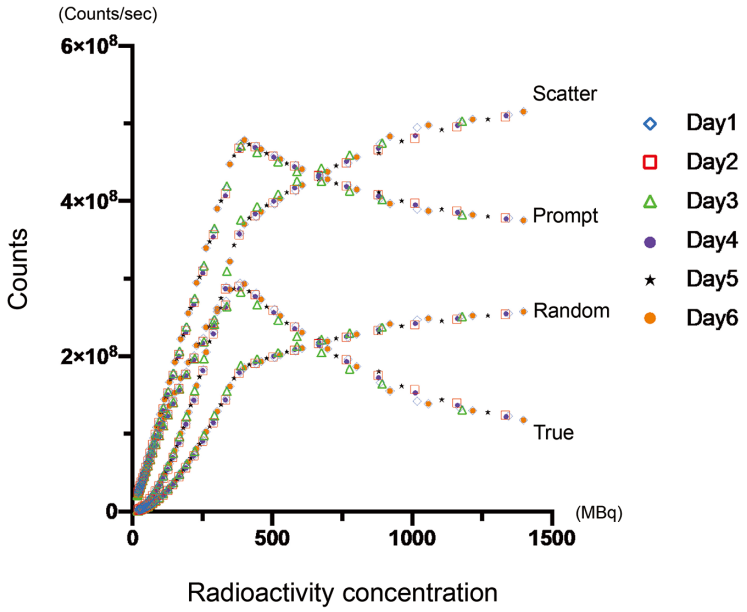

Figure 3　Counting rate performance of mCT scanner for ^{13}N.
The scatter, prompt, random, and true counts derived from all sessions for 6 days were plotted. The curve profile of true counts showed its peak on approximately 300 Mcps, corresponding approximately 360 MBq. Each color and sign indicated 1 to 6 day of sessions as shown in right side of the graph.

theoretical value of 400 MBq, while the dose-dependency appeared to be maintained. However, the theoretical dose over 740 MBq showed a markedly dispersion of the plots, and the actual values has started to drop. This deceasing trend of measured value for higher dose was obvious for the day 1, 2, and 4, while the dose-dependency appeared to be maintained for day 2, 3, and 5. The measured values for day 2, 3, and 5 appeared to show wider SD value. A simple linear regression analysis demonstrated a good correlation in a range of theoretical dose below 370 MBq (r^2=1.0 ± 0.0001, p<0.0001 for all sets), and 370 to 740 MBq (r^2=0.99 ± 0.0001, p<0.0001 for all sets), while did not show a statistical significance in the range over 740 MBq (p=0.62). As shown in graph of Figure 3, scatter, prompt, random, and true counts derived from all sessions for 6 days were plotted and demonstrated that the true counts showed its peak on approximately 300 Mcps, corresponding approximately 360 MBq on radioactive concentration in phantom. Figure 4 showed the plotted curves of mean net true count rates and random count rates for all sessions. Net true counts rate showed its peak at mean 4.8 Mpcs and started to drop, where the corresponding theoretical value was 36.3 MBq/mL. The plots of random counts rate showed marked steep in higher activities, but showed the trend of less steep over 2.9 Mcps. NECR showed highest in its peak in mean 3.0 Mcps, and the corresponding theoretical activity in the phantom was 36.3 MBq/mL.

Discussion

In this study, we preliminarily evaluated the effect of count-loss on the IF calculation using simplified phantom model imitating small ventricle, and estimated the optimal radioactivity for ^{13}N ammonia dynamic perfusion using high-resolution scanner. Our decaying-source experiment using simplified-cylindrical phantom showed that the PET performance of measuring radioactive concentration in left ventricle was significantly limited in high-dose of ^{13}N. In the present study, the theoretical dose and measured activity showed the discrepancy among the sessions for the dose over 740 MBq, indicating the limitation of the reproducibility due to count loss. The maximum NECR was obtained with theoretical radioactive concentration of 36.3 MBq/mL. If the radioactivity of vial at the value of 95% of the maximum NECR was defined as optimal, because of the plateau like nature, approximately up to 45 MBq/mL can be suggested as acceptable upper limit of radioactivity for accurate IF estimation (12). However, when considering radioactive tracer is promptly diluted during the delivery from the peripheral vein into the left ventricle, the radioactivity in left ventricle should be greatly less than the administrated dose (e.g., less than 360 MBq in 10 mL, or 740 MBq in 20 mL if the patient with small heart is assumed). American society of nuclear cardiology suggested the recommended dose of ^{13}N as up to 740 MBq (13). Although our result indicated that there was a risk of increased count-loss when using highest dose for small heart, our data also suggested that the routine dose up to 740 MBq in clinical setting was still reproducible for IF calculation in clinical practice.

The impact of high dose injections on flow quantification

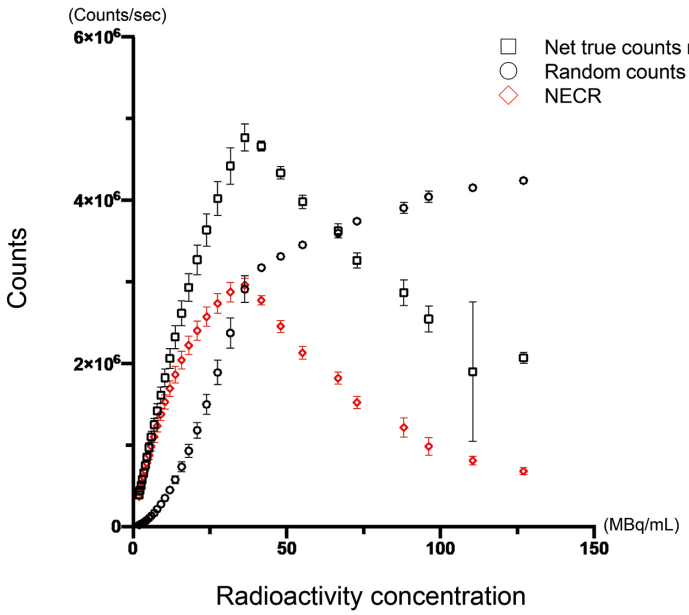

Figure 4 Count rate measurement of ^{13}N.

The relation of measured radioactivity and count rate from PET acquisition was shown. The graph for random coincidence counts rate (circle) and net true count rate (square). X-axis indicated the theoretical radioactive concentration (MBq/mL) estimated by the radioactive decay from the measured activity in the vial obtained by curie meter prior to PET scan. Y-axis indicated the count rate (counts/sec) of the vial from the PET acquisitions. The inclination of the graph for random coincidence counts rate started to decrease at the plot of approximately 3 Mcps (approximately 36.3 MBq/mL for estimated radioactive concentration). Net true counts rate demonstrated its peak for below 4.8 Mcps (approximately 36 MBq for estimated radioactive concentration). The plots for NECR. The definition of X and Y-axis was similar to graph A. NECR analysis showed the peak for approximately 3.0 Mcps (36.3 MBq/mL for estimated radioactive concentration).

should be discussed particularly for short half-life PET tracers such as ^{15}O, ^{82}Rb, and ^{13}N, albeit the feasibility study of reducing the dose has been challenging *in vivo*. Tout et al. investigated in the clinical cases for ^{82}Rb, reported that there was evidence of detector saturation when first-pass dynamic study with 1480 MBq, namely there has been significant risk for count-loss for ^{82}Rb dynamic studies in calculating IF (14). Lassen et al. compared the repeated scans with half and full dose of ^{82}Rb (662 ± 115 MBq for half-dose), and reported that the saturation effect was not observed in half dose scan, while 20% of full dose scan demonstrated that effects (15). Lassen et al. also investigated the feasibility of reduced injected dose. They compared full, half, and quarter dose from simulative reduction by reconstruction from routine list-mode scan (estimated quarter dose was 290 ± 50 MBq), and reported the qualitative scoring for perfusion defect was comparable among the doses. However, they found the simulated quoter dose significantly reduced contrast-to-noise ratio, and increased blood pool noise, resulting reduced diagnostic accuracy (16). However, there is no clinical investigation using ^{13}N for reducing dose. It is speculated that the visual interpretation for static image is maintained due to high-resolution technique such as TOF (3, 17).

In the phantom studies, Bui et al. employed their original circulating arterial phantom model, and reported that 2 min of 3D acquisition with ^{82}Rb dose over 1147 MBq significantly underestimated arterial input function (4). However, the tube phantom for sampling input function they employed was 1,000 mL imitating Aorta, and 2-min acquisition for dynamic scan. Since most dedicated software packages for MBF calculation are standardized to place region of interest in left ventricular (LV) cavity to obtain TAC. The actual interval of perfusion tracer passing through LV in clinical dynamic study should be approximately less than two minutes (18), and this was the primal reason that the acquisition timing was set as 60 sec in our study. Other phantom study for ^{82}Rb, Renaud et al. reported that approximately 3 to 14 MBq/kg dose of radioactivity is recommended as injected dose, and the counting rate should be 4 to 14 Mcps as recommendation (19). They used standard cardiac phantom for IF, myocardial flow, and uptake simulation, namely the chamber size was larger than that of our model. O'Doherty et al. using PETMR system with flow-controlled perfusion phantom, employed ^{18}F of similar radioactivity to the present study and reported that NECR was maintained at 34.1 Mcps, corresponding to 310 MBq in the phantom of 120 mL (10). All those studies were well-

designed, enrolled standard or in-house original phantoms emulating cardiac chamber to simulate the dynamic study. However, all phantoms were sized over 100 mL, assuming the chamber volume in end-diastole phase of normal western population (i.e., 100 ± 19 mL for healthy female) (20). Zhang Z et al. reported that the reference value of endo-systolic LV volume in healthy Chinese women was 22.1 ± 6.1 for aged over 60 (21). Furthermore, LV size should be smaller for low body mass index or children, and the reproducibility of MBF calculation needs to be discussed for such patients. The NECR evaluation in the present study also has a potential for estimating count-loss for pediatric studies. The failure in performance at higher activities in small volume is due to increasing counting losses and accidental coincidences. Hence, it is difficult to refer above previous phantom studies for the simulation of count-loss in dynamic study with small LV cavity. This is a first preliminary study to estimate counts rate for perfusion tracer in small-sized heart. In clinical validation study, Vasquez AF et al. investigated the feasibility of flow quantification employing various anatomic IF including left ventricle, multiple sites of aorta, and left atrium. They found the variety of IF among different arterial sites had significant impact on flow calculation. IF derived from LV was significantly affected by the spillover and misregistration due to frequent motion, resulting overestimation of myocardial flow (22). The present study did not simulate the anatomical site for IF, thus further analysis for the location and size of region of interest in is needed, simulating frequent cardiac motion with free breathing.

This study has several limitations. First, the optimal radioactivity obtained in the current study is still challenging convert to the optimal injected dose in clinical setting. Second, the size of LV for small heart has been underestimated in SPECT studies, thus the true LV cavity should be larger from other imaging modalities such as magnetic resonance imaging (23). Third, we did not enroll the reframing for dynamic series from list-mode data because the estimation of count-loss using NECR was the primal aim of this study, thus count profile was not perfectly interchangeable to the clinical study. The limitation of NECR estimate should be also discussed. NECR does not account for possible counting rate dependent bias, attenuation correction, or reconstruction. We did not evaluate signal to nose ratio in this study because we used neck phantom without imitated surrounding organs. As shown in Figure 2, a measured activity was markedly varied in higher dose over 740 MBq, and the variation was obvious among sessions. The potential reasons for this variation were the manual volume of interest setting, and location of the phantom, causing the dispersion in the scatter plots for the higher dose. Thus, despite these limitations, the NECR analysis successfully characterized count-loss phenomenon in small heart.

Conclusion

Simulative analysis with phantom mimicking end-systolic LV cavity of small heart confirmed that considerable count-loss can occur for high-dose of ^{13}N. This result can be useful information in assessing the feasibility of IF calculation in clinical myocardial perfusion PET.

Acknowledgments

None.

Sources of funding

None.

Conflicts of interest

None.

Reprint requests and correspondence:
Kenji Fukushima, MD, PhD
Department of Radiology and Nuclear Medicine, Fukushima Medical University
Hikarigaoka-1, Fukushima city, Fukushima, Japan
E-mail: kfukush4@fmu.ac.jp

References

1. Murthy VL, Bateman TM, Beanlands RS, Berman DS, Borges-Neto S, Chareonthaitawee P, et al. Clinical quantification of myocardial blood flow using PET: Joint position paper of the SNMMI cardiovascular council and the ASNC. J Nucl Med 2018; 59: 273–93.
2. Suda M. Benefits of time-of-flight positron emission tomography computed tomography with ^{13}N-ammonia. Ann Nucl Cardiol 2016; 2: 188–91.
3. Matsuo S, Mochizuki T, Takeda S, Shibutani T, Onoguchi M, Nakajima K, et al. Cardiac time-of-flight PET for evaluating myocardial perfusion with ^{13}N-ammonia: Phantom studies for estimation of defect and heterogeneity. Ann Nucl Cardiol 2016; 2: 73–8.
4. Bui L, Kitkungvan D, Roby AE, Nguyen TT, Gould KL. Pitfalls in quantitative myocardial PET perfusion II: Arterial input function. J Nucl Cardiol 2020; 27: 397–409.
5. Nakajima K, Okuda K, Nyström K, Richter J, Minarik D, Wakabayashi H, et al. Improved quantification of small hearts for gated myocardial perfusion imaging. Eur J Nucl Med Mol Imaging 2013; 40: 1163–70.
6. Badawi RD, Miller MP, Bailey DL, Marsden PK. Randoms variance reduction in 3D PET. Phys Med Biol 1999; 44: 941–54.
7. Strother SC, Casey ME, Hoffman EJ. Measuring PET scanner sensitivity: Relating countrates to image signal-to-noise ratios using noise equivalents counts. IEEE Transactions on Nuclear Science 1990; 37: 783–8.

8. Shimada N, Daisaki H, Murano T, Terauchi T, Shinohara H, Moriyama N. Optimization of the scan time is based on the physical index in FDG-PET/CT. Nihon Hoshasen Gijutsu Gakkai Zasshi 2011; 67: 1259–66. [Article in Japanese]
9. Wang GC, Li X, Niu X, Du H, Balakrishnan K, Ye H, et al. PET timing performance measurement method using NEMA NEC phantom. IEEE Transactions on Nuclear Science 2016; 63: 1335–42.
10. O'Doherty J, Sammut E, Schleyer P, Stirling J, Nazir MS, Marsden PK, et al. Feasibility of simultaneous PET-MR perfusion using a novel cardiac perfusion phantom. Eur J Hybrid Imaging 2017; 1: 4.
11. Tatsuno K, Okuda K, Nakajima K, Saito H, Shibutani T, Onoguchi M, et al. Normal and range value evaluations using heart risk view-function based on the Japanese Society of Nuclear Medicine working group database. Ann Nucl Cardiol 2022; 8: 51–6.
12. Walker MD, Matthews JC, Asselin MC, Saleem A, Dickinson C, Charnley N, et al. Optimization of the injected activity in dynamic 3D PET: A generalized approach using patient-specific NECs as demonstrated by a series of ^{15}O-H_2O scans. J Nucl Med 2009; 50: 1409–17.
13. Murthy VL, Bateman TM, Beanlands RS, Berman DS, Borges-Neto S, Chareonthaitawee P, et al. Clinical quantification of myocardial blood flow using PET: Joint position paper of the SNMMI Cardiovascular Council and the ASNC. J Nucl Cardiol 2018; 25: 269–97.
14. Tout D, Tonge CM, Muthu S, Arumugam P. Assessment of a protocol for routine simultaneous myocardial blood flow measurement and standard myocardial perfusion imaging with rubidium-82 on a high count rate positron emission tomography system. Nucl Med Commun 2012; 33: 1202–11.
15. Lassen ML, Manabe O, Otaki Y, Eisenberg E, Huynh P, Wang F, et al. 3D PET/CT ^{82}Rb PET myocardial blood flow quantification: Comparison of half-dose and full-dose protocols. Eur J Nucl Med Mol Imaging 2020; 47: 3084–93.
16. Lassen ML, Otaki Y, Kavanagh P, Miller RJH, Berman DS, Slomka PJ. Simulation of low-dose protocols for myocardial perfusion ^{82}Rb imaging. J Nucl Med 2021; 62: 1112–7.
17. DiFilippo FP, Brunken RC. Impact of time-of-flight reconstruction on cardiac PET images of obese patients. Clin Nucl Med 2017; 42: e103–8.
18. Vidula MK, Selvaraj S, Guerraty MA. Cardiopulmonary transit time: Reinforcing the case for positron emission tomography after heart transplantation. J Nucl Cardiol 2022; 29: 1245–7.
19. Renaud JM, Yip K, Guimond J, Trottier M, Pibarot P, Turcotte E, et al. Characterization of 3-dimensional PET systems for accurate quantification of myocardial blood flow. J Nucl Med 2017; 58: 103–9.
20. Boyd HL, Rosen SD, Rimoldi O, Cunningham VJ, Camici PG. Normal values for left ventricular volumes obtained using gated PET. G Ital Cardiol 1998; 28: 1207–14.
21. Zhang Z, Ma Q, Gao Y, Cao L, Zhu C, Zhao Z, et al. Biventricular morphology and function reference values derived from a large sample of healthy Chinese adults by magnetic resonance imaging. Front Cardiovasc Med 2021; 8: 697481.
22. Vasquez AF, Johnson NP, Gould KL. Variation in quantitative myocardial perfusion due to arterial input selection. JACC Cardiovasc Imaging 2013; 6: 559–68.
23. Okuda K, Nakajima K. Normal values and gender differences of left ventricular functional parameters with cardioREPO software: Volume, diastolic function, and phase analysis. Ann Nucl Cardiol 2017; 3: 29–33.